

# The Charge Form Factor of the Neutron at Low Momentum Transfer from the ${}^2\vec{H}(\vec{e}, e'n)p$ Reaction

E. Geis,<sup>1,\*</sup> M. Kohl,<sup>2,†</sup> V. Ziskin,<sup>2,\*</sup> T. Akdogan,<sup>2</sup> H. Arenhövel,<sup>3</sup> R. Alarcon,<sup>1</sup> W. Bertozzi,<sup>2</sup> E. Booth,<sup>4</sup> T. Botto,<sup>2</sup> J. Calarco,<sup>5</sup> B. Clasio,<sup>2</sup> C.B. Crawford,<sup>2</sup> A. DeGrush,<sup>2</sup> T.W. Donnelly,<sup>2</sup> K. Dow,<sup>2</sup> M. Farkhondeh,<sup>2</sup> R. Fatemi,<sup>2</sup> O. Filoti,<sup>5</sup> W. Franklin,<sup>2</sup> H. Gao,<sup>6</sup> S. Gilad,<sup>2</sup> D. Hasell,<sup>2</sup> P. Karpus,<sup>5</sup> H. Kolster,<sup>2</sup> T. Lee,<sup>5</sup> A. Maschinot,<sup>2</sup> J. Matthews,<sup>2</sup> K. McIlhany,<sup>7</sup> N. Meitanis,<sup>2</sup> R.G. Milner,<sup>2</sup> J. Rapaport,<sup>8</sup> R.P. Redwine,<sup>2</sup> J. Seely,<sup>2</sup> A. Shinozaki,<sup>2</sup> S. Širca,<sup>2</sup> A. Sindile,<sup>5</sup> E. Six,<sup>1</sup> T. Smith,<sup>9</sup> M. Steadman,<sup>2</sup> B. Tonguc,<sup>1</sup> C. Tschalaer,<sup>2</sup> E. Tsentalovich,<sup>2</sup> W. Turchinets,<sup>2</sup> Y. Xiao,<sup>2</sup> W. Xu,<sup>6</sup> C. Zhang,<sup>2</sup> Z. Zhou,<sup>2</sup> and T. Zwart<sup>2</sup>

(The BLAST Collaboration)

<sup>1</sup>Arizona State University, Tempe, AZ 85287

<sup>2</sup>Laboratory for Nuclear Science and Bates Linear Accelerator Center, Massachusetts Institute of Technology, Cambridge, MA 02139

<sup>3</sup>Institut für Kernphysik, Johannes Gutenberg-Universität Mainz, D-55099 Mainz, Germany

<sup>4</sup>Boston University, Boston, MA 02215

<sup>5</sup>University of New Hampshire, Durham, NH 03824

<sup>6</sup>Triangle Universities Nuclear Laboratory and Duke University, Durham, NC 27708-0305

<sup>7</sup>United States Naval Academy, Annapolis, MD 21402

<sup>8</sup>Ohio University, Athens, OH 45701

<sup>9</sup>Dartmouth College, Hanover, NH 03755

(Dated: October 22, 2018)

We report new measurements of the neutron charge form factor at low momentum transfer using quasielastic electrodisintegration of the deuteron. Longitudinally polarized electrons at an energy of 850 MeV were scattered from an isotopically pure, highly polarized deuterium gas target. The scattered electrons and coincident neutrons were measured by the Bates Large Acceptance Spectrometer Toroid (BLAST) detector. The neutron form factor ratio  $G_E^n/G_M^n$  was extracted from the beam-target vector asymmetry  $A_{ed}^V$  at four-momentum transfers  $Q^2 = 0.14, 0.20, 0.29$  and  $0.42$  (GeV/c)<sup>2</sup>.

PACS numbers: 13.40.-f, 13.40.Gp, 13.88.+e, 14.20.Dh, 25.30.Bf

Keywords: Neutron, form factor, polarization, internal target, elastic, deuterium

The neutron is composed of charged constituents, whose net distribution is described by the charge (or electric) form factor  $G_E^n$ . Differences in the up and down quark distributions produce a nonuniform distribution of the net charge [1]. The neutron electric form factor  $G_E^n$  exhibits a maximum in the region of  $Q^2 \approx 0.1 - 0.5$  (GeV/c)<sup>2</sup>; when Fourier-transformed this corresponds to a positively charged core and a concentration of negative charge at intermediate to large distances of  $\approx 1$  fm, commonly associated with a meson cloud surrounding the nucleon. Models which emphasize the role of the meson cloud have been successful in explaining important aspects of nucleon structure [2, 3, 4, 5, 6]. Precise knowledge of  $G_E^n$  is essential for the description of electromagnetic structure of nuclei, and for the interpretation of parity violating electron scattering experiments to determine the strangeness content of the nucleon. Further, it is anticipated that exact *ab initio* QCD calculations of  $G_E^n$  using lattice techniques will eventually be possible [7].

In the absence of a free neutron target, determinations of  $G_E^n$  at finite  $Q^2$  are typically carried out using quasielastic electron scattering from deuterium or <sup>3</sup>He targets. Despite the small value of  $G_E^n$  compared to the

neutron magnetic form factor  $G_M^n$ , it can be obtained with high precision from double-polarization observables based on the interference of  $G_E^n$  with  $G_M^n$ . With the availability of high-duty-factor polarized electron beams over the last decade, experiments have employed recoil polarimeters, and targets of polarized <sup>2</sup>H and <sup>3</sup>He to perform precision measurements of  $G_E^n$  using polarization techniques with inherently small systematic uncertainties [8]. The slope of  $G_E^n(Q^2)$  at  $Q^2 = 0$ , which defines the square of the neutron charge radius, is determined precisely by the scattering of thermal neutrons from atomic electrons [9].

This paper reports on new measurements of  $G_E^n/G_M^n$  at low  $Q^2$  in the vicinity of the maximum of  $G_E^n$ , using a longitudinally polarized electron beam incident on a vector-polarized <sup>2</sup>H target internal to the South Hall Ring at the MIT-Bates Linear Accelerator Center. The BLAST detector was used to detect quasielastically scattered electrons in coincidence with recoil neutrons over a range of  $Q^2$  between 0.10 and 0.55 (GeV/c)<sup>2</sup>.

The differential cross section for the <sup>2</sup>H(e, e'n) reaction with polarized beam and target can be written [10, 11, 12]

$$d^3\sigma/(d\Omega_e d\Omega_{pq} d\omega) = \sigma_{unp}(1 + \Sigma + P_e \Delta) \quad (1)$$

with

$$\begin{aligned}\Sigma &= \sqrt{\frac{3}{2}}P_z A_d^V + \sqrt{\frac{1}{2}}P_{zz} A_d^T \\ \Delta &= A_e + \sqrt{\frac{3}{2}}P_z A_{ed}^V + \sqrt{\frac{1}{2}}P_{zz} A_{ed}^T,\end{aligned}\quad (2)$$

where  $\sigma_{unp}$  is the unpolarized differential cross section,  $P_z = n_+ - n_-$  and  $P_{zz} = n_+ + n_- - 2n_0$  are the vector and tensor polarizations of the deuteron target defined by the relative populations  $n_m$  of the three deuteron magnetic substates with respect to the deuteron orientation axis,  $m = +1, 0, -1$ , respectively, and  $P_e$  is the longitudinal polarization of the electron beam.

With BLAST, all of the polarization observables  $A_i$  in Eq. (2) have been measured for the first time with precision in a single experiment. The beam-target vector polarization observable  $A_{ed}^V$  is particularly sensitive to the neutron form factor ratio  $G_E^n/G_M^n$  [12]. In the Plane Wave Born Approximation (PWBA) and with the deuteron in a pure S-state, the asymmetry  $A_{ed}^V$  can be written analogously to elastic scattering from the free neutron as

$$\begin{aligned}A_{ed}^V &= \frac{a G_M^n{}^2 \cos \theta^* + b G_E^n G_M^n \sin \theta^* \cos \phi^*}{c G_E^n{}^2 + G_M^n{}^2} \\ &\approx a \cos \theta^* + b \frac{G_E^n}{G_M^n} \sin \theta^* \cos \phi^*,\end{aligned}\quad (3)$$

where  $\theta^*$  and  $\phi^*$  are the target spin orientation angles with respect to the momentum transfer vector and  $a$ ,  $b$ , and  $c$  are known kinematic factors. This asymmetry has the largest sensitivity to  $G_E^n$  when the momentum transfer vector is perpendicular to the target polarization, *i.e.*  $\theta^* = 90^\circ$ .

However, there are sizable corrections to the asymmetry in Eq. (3), mainly at low  $Q^2$  where they are dominated by final state interactions (FSI). The relative contributions of meson exchange currents (MEC), isobar configurations (IC) and relativistic corrections (RC) become more significant as the momentum transfer increases (see Fig. 1). Extracting  $G_E^n$  must be done by comparison with theoretical asymmetries that include these effects.

The effects of FSI can be monitored with the other polarization observables in Eq. (2). The asymmetries  $A_e$ ,  $A_d^T$ , and  $A_{ed}^T$  all vanish in the Born approximation due to parity and time reversal conservation and remain very small (below 1%) even in the presence of FSI. This permits these observables to be used to identify any false asymmetries in the experiment. FSI gives a sizable contribution to the target tensor asymmetry  $A_d^T$ , which is insensitive to  $G_E^n$  and otherwise close to zero in the quasifree limit. Figure 1 displays a Monte Carlo simulation of the reaction mechanism effects on the asymmetries  $A_{ed}^V$  (upper panel) and  $A_d^T$  (lower panel) as a function of  $Q^2$  along with the measured values.

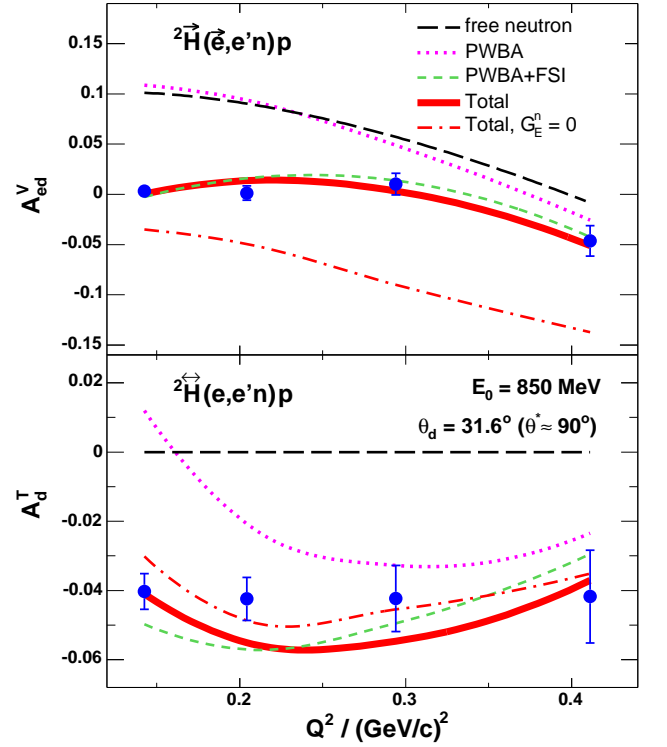


FIG. 1: Measured (solid blue points) and calculated beam-target vector polarization observable  $A_{ed}^V$  (upper panel) and tensor asymmetry  $A_d^T$  (lower panel) for the  ${}^2\text{H}(e, e'n)p$  reaction at 850 MeV, a target orientation of  $\theta_d = 31.6^\circ$  into the left sector of BLAST, and with neutrons detected in the right sector. The colored curves are Monte Carlo simulations based on the deuteron electrodisintegration model of Ref. [11] (dotted magenta = PWBA, short-dashed green = PWBA+FSI, solid red = PWBA+FSI+MEC+IC+RC) using standard parameterizations for the nucleon form factors (see text). In addition, the corresponding curves for  $G_E^n \equiv 0$  (dash-dotted red) and for elastic scattering from the free neutron (dashed black line) are shown.

The calculations use the standard dipole form factor  $G_D = (1 + Q^2/0.71)^{-2}$  for  $G_E^p$ ,  $G_M^p/\mu_p$ , and  $G_M^n/\mu_n$ , and  $1.91\tau/(1 + 5.6\tau)G_D$  for  $G_E^n$  [13], where  $\mu_p = 2.79$ ,  $\mu_n = -1.91$ , and  $\tau = Q^2/(4m_n^2)$ . The good agreement of the measured tensor asymmetry  $A_d^T$  with the full model supports the calculations of FSI for a reliable extraction of  $G_E^n$  from the beam-target vector asymmetry  $A_{ed}^V$  at the percent level.

On the other hand, the corrections at low  $Q^2$  to  $A_{ed}^V$  measured in the  ${}^2\vec{\text{H}}(\vec{e}, e'p)n$  reaction in quasifree kinematics are negligible [12], which allows for a precise determination of the product of beam and target polarizations  $P_e P_z$  along with the proton form factor ratio  $G_E^p/G_M^p$  in this reaction channel [14].

The BLAST experiment was designed to carry out spin-dependent electron scattering from hydrogen [15] and light nuclei. Details on the experimental setup can be found in [16]. The internal target consisted of an

atomic beam source (ABS) combined with an open-ended storage cell through which the stored electron beam passed continuously [17]. The ABS produced polarized monoatomic deuterium gas in the storage cell with nuclear vector ( $V+$ :  $m=1$ ;  $V-$ :  $m=-1$ ) and tensor ( $T-$ :  $m=0$ ) polarization states. In addition, the helicity  $h$  of the electron beam was flipped every injection cycle. Linear combinations of the six charge-normalized yields  $Y_{hm}$  define all five polarization observables in Eq. (2). The experimental value of the beam-vector polarization observable  $A_{ed}^V$  can be written as

$$A_{ed}^V = \sqrt{\frac{3}{2}} \frac{1}{P_e P_z} \frac{Y_{++} + Y_{--} - Y_{+-} - Y_{-+}}{Y_{tot}}, \quad (4)$$

where  $Y_{tot}$  is the total yield obtained by summing up all six combinations  $hm$ . A modest magnetic holding field was applied to define the polarization angle  $\theta_d$  within the horizontal plane and to minimize the depolarization of target atoms. The variation of  $\theta_d$  was carefully mapped over the extent of the target cell. The average value of  $\theta_d$  was determined along with the tensor polarization  $P_{zz}$  by comparing the simultaneously measured tensor asymmetries in elastic scattering from tensor-polarized deuterium [18] with those expected at low  $Q^2$  based on a parameterization of previous data [19].

The BLAST detector is a toroidal spectrometer (8 sectors) with the horizontal sectors instrumented with wire chambers, aerogel Čerenkov counters, thin plastic timing scintillators, and thick plastic scintillator walls for neutron detection. With the target polarization vector pointing into the left sector, the neutron detection efficiency was augmented in the right sector covering the kinematic region most sensitive to the neutron form factor ratio, as indicated by the  $\sin \theta^*$  term in Eq. (3). The detection of neutrons in the left sector was primarily used to independently verify the determination of  $P_e P_z$  from the  ${}^2\bar{H}(\vec{e}, e'p)n$  reaction.

The selection of  $(e, e'n)$  events is very clean; the number of proton tracks misidentified as neutrons is negligible, due to the highly efficient charged particle veto provided by the thin scintillator bars and the large-volume drift chambers in front of the neutron detectors. A set of cuts applied on the time correlation between the charged and the neutral track, and on kinematic constraints for the electrodisintegration process, was employed to identify the quasielastic  $(e, e'n)$  events. The background from scattering off the aluminum target cell walls, measured with a hydrogen (empty) target, is less than 4% (3%) of the normalized yield obtained with deuterium.

The corrected asymmetries were compared to Monte Carlo simulations based on the deuteron electrodisintegration model [11], for which events were generated according to the unpolarized cross section and weighted event-by-event with the spin-dependent terms in Eq. (2). The acceptance-averaged asymmetry  $A_{ed}^V$  was simulated

for different values of  $G_E^n/G_M^n$  and compared to the experimental values. In order to extract the best value of the form factor ratio for each  $Q^2$  bin, a  $\chi^2$  minimization was performed independently with respect to the missing momentum of the reaction and the angle of the neutron in the hadronic center-of-mass system. Both extractions produced consistent results.

The data reported here were acquired in two separate runs in 2004 and 2005, corresponding to a target polarization angle of  $31.64^\circ \pm 0.43^\circ$  and  $46.32^\circ \pm 0.45^\circ$ , respectively. With a total accumulated beam charge of 451 kC (503 kC) in the first (second) data set, final samples of 268,914 (205,252) coincident electron-neutron events were collected. The average product of beam and target polarization determined from the  ${}^2\bar{H}(\vec{e}, e'p)$  reaction was  $P_e P_z = 0.5796 \pm 0.0034(\text{stat}) \pm 0.0034(\text{sys})$  in the first and  $0.5149 \pm 0.0043(\text{stat}) \pm 0.0054(\text{sys})$  in the second data set [14]. In comparison, the polarization product determined from  ${}^2\bar{H}(\vec{e}, e'n)p$  with neutrons detected in the left sector of BLAST corresponding to  $\theta^* \approx 0^\circ$ , was found to be  $0.587 \pm 0.019(\text{stat})$  and  $0.481 \pm 0.026(\text{stat})$  consistent with the above  $(e, e'p)$  results. The two data sets were treated as separate experiments producing two consistent results for the form factor ratio, which were combined for a final result. The data were divided into four  $Q^2$  bins to determine  $G_E^n/G_M^n$  with a comparable statistical significance (see Table I).

The systematic error of  $G_E^n/G_M^n$  is dominated by the uncertainty of the target spin angle  $\theta_d$ . Other systematic uncertainties include that of the beam-target polarization product  $P_e P_z$ , the accuracy of kinematic reconstruction, as well as the dependency on software cuts. The systematic uncertainties were evaluated individually for each  $Q^2$  bin and data set by combining the errors from each source, taking covariances into account; the correlated and uncorrelated error categories of the two measurements were then combined for a resulting systematic error of each bin. False asymmetries were studied with the observables  $A_d^V$  and  $A_{ed}^T$  and found to be consistent with zero. Radiative corrections to the asymmetries calculated in a PWBA formalism using the code MASCARAD [20] are  $<1\%$  and therefore also neglected. The uncertainties of the reaction mechanism and FSI corrections, which are small compared to the experimental errors, are not included in the systematic error.

$Q^2/(\text{GeV}/c)^2$	$\langle Q^2 \rangle/(\text{GeV}/c)^2$	$\mu_n G_E^n/G_M^n$
0.10–0.17	0.142	$0.0505 \pm 0.0072 \pm 0.0031$
0.17–0.25	0.203	$0.0695 \pm 0.0084 \pm 0.0039$
0.25–0.35	0.291	$0.1022 \pm 0.0127 \pm 0.0046$
0.35–0.55	0.415	$0.1171 \pm 0.0182 \pm 0.0052$

TABLE I: Results for the extracted neutron form factor ratio  $\mu_n G_E^n/G_M^n$  ( $\mu_n = G_M^n(0) = -1.91$ ) with statistical and systematic errors, respectively.

The world's data on  $G_E^n$  from double-polarization experiments [8] are displayed in Fig. 2 along with the results of this work. All of the polarization data were experimentally determined as electric to magnetic form factor ratios. We used parameterization [21] for  $G_M^n$ , which is in good agreement with recent measurements [22], to determine  $G_E^n$  from BLAST and to adjust the previously published values. The data from a variety of experiments are consistent and remove the large model uncertainty of previous  $G_E^n$  extractions from elastic electron-deuteron scattering [23]. The new distribution is also in agreement with  $G_E^n$  extracted from the deuteron quadrupole form factor [24].

The measured distribution of  $G_E^n$  can be parameterized as a function of  $Q^2$  based on the sum of two dipoles,  $\sum_i a_i/(1+Q^2/b_i)^2$  ( $i=1,2$ ), shown as the BLAST fit in Fig. 2 (blue line) with a one-sigma error band. With  $G_E^n(0) = 0$  and the slope at  $Q^2 = 0$  constrained by  $\langle r_n^2 \rangle = (-0.1148 \pm 0.0035) \text{ fm}^2$  [9], one parameter is fixed, resulting in  $a_1 = -a_2 = 0.095 \pm 0.018$ ,  $b_1 = 2.77 \pm 0.83$ ,  $b_2 = 0.339 \pm 0.046$  and  $\text{cov}(a_1, b_1) = -0.014$ ,  $\text{cov}(a_1, b_2) = 0.0008$ ,  $\text{cov}(b_1, b_2) = -0.036$  with  $Q^2$  in units of  $(\text{GeV}/c)^2$ . The parameterization [25] (magenta dash-dotted line) is based on the form introduced in [21] with an additional bump structure around  $0.2 - 0.4 (\text{GeV}/c)^2$ . Also shown are recent results based on vector meson dominance (VMD) and dispersion relations (red short-dashed [4] and green long-dashed lines [5]), and the prediction of a light-front cloudy bag model with relativistic constituent quarks [6] (cyan dotted line).

The new data from BLAST do not show a bump structure at low  $Q^2$  as previously suggested [21, 25]. The BLAST data are in excellent agreement with VMD based models [4, 5] and also agree with the meson-cloud calculation [6]. The improved precision of the data at low  $Q^2$  provides strong constraints on the theoretical understanding of the nucleon's meson cloud.

We thank the staff of the MIT-Bates Linear Accelerator Center for delivering high quality electron beam and for their technical support, and A. Bernstein for suggesting the form of the BLAST fit. This work has been supported in part by the US Department of Energy and National Science Foundation.

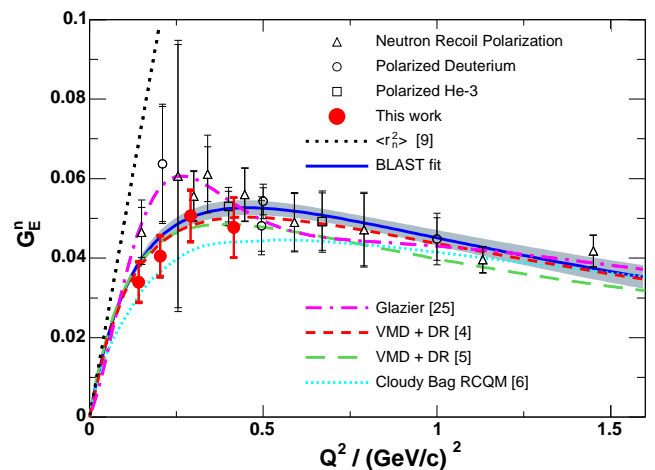


FIG. 2: World data on  $G_E^n$  from double-polarization experiments [8]. The data correspond to neutron recoil polarization experiments with unpolarized  $^2\text{H}$  target (open triangles) and experiments with polarized  $^2\text{H}$  (open circles; solid red dots = this work) and  $^3\text{He}$  targets (open squares). The data are shown with statistical (small error bars) and with statistical and systematic errors added quadratically (large error bars). The “BLAST fit” (blue solid line) is a parameterization of the data based on the sum of two dipoles shown with a one-sigma error band. The recent parameterization [25] (magenta dash-dotted line) is based on the form introduced in [21]. Also shown are recent results based on vector meson dominance and dispersion relations (red short-dashed [4] and green long-dashed lines [5]), and of a light-front cloudy bag model with relativistic constituent quarks [6] (cyan dotted line).

- [5] M.A. Belushkin, H.-W. Hammer, and Ulf-G. Meißner, Phys. Rev. C **75**, 035202 (2007).  
 [6] G.A. Miller, Phys. Rev. C **66**, 032201(R) (2002).  
 [7] C. Alexandrou, G. Koutsou, J.W. Negele, and A. Tsapalis, Phys. Rev. D **74**, 034508 (2006).  
 [8] B. Plaster *et al.*, Phys. Rev. C **73**, 025205 (2006) and references therein.  
 [9] S. Kopecky *et al.*, Phys. Rev. Lett. **74**, 2427 (1995); Phys. Rev. C **56**, 2229 (1997).  
 [10] T.W. Donnelly and A.S. Raskin, Ann. Phys. **169**, 247 (1986).  
 [11] H. Arenhövel, W. Leidemann, and E.L. Tomusiak, Eur. Phys. J. A **23**, 147 (2005); Phys. Rev. C **46**, 455 (1992).  
 [12] H. Arenhövel, W. Leidemann, and E.L. Tomusiak, Z. Phys. A **331**, 123 (1988); Erratum Z. Phys. A **334**, 363 (1989).  
 [13] S. Galster *et al.*, Nucl. Phys. **B32**, 221 (1971).  
 [14] A. Maschinot, Ph.D. thesis, Massachusetts Institute of Technology, 2005; A. DeGrush, Ph.D. thesis, Massachusetts Institute of Technology, in preparation; A. DeGrush *et al.*, to be published.  
 [15] C.B. Crawford *et al.*, Phys. Rev. Lett. **98**, 052301 (2007).  
 [16] D. Hasell *et al.*, The BLAST Experiment (to be published).  
 [17] D. Cheever *et al.*, Nucl. Instrum. Methods Phys. Res., Sect. A **556**, 410 (2006); L.D. van Buuren *et al.*, Nucl. Instrum. Methods Phys. Res., Sect. A **474**, 209 (2001).  
 [18] C. Zhang, Ph.D. thesis, Massachusetts Institute of Tech-

\* Reported results are based on the Ph.D. theses of E.G. and V.Z.

† Corresponding author, email kohlm@jlab.org

- [1] A. Thomas and W. Weise, *The Structure of the Nucleon* (Wiley-VCH, Berlin, 2001).  
 [2] Z. Dziembowski *et al.*, Ann. Phys. **258**, 1 (1997).  
 [3] B. Pasquini and S. Boffi, Phys. Rev. D **76**, 074011 (2007).  
 [4] E.L. Lomon, Phys. Rev. C **64** 035204 (2001); Phys. Rev. C **66**, 045501 (2002); arXiv:nucl-th/0609020v2; to be published and private communication.

- nology, 2006; C. Zhang *et al.*, to be published.
- [19] D. Abbott *et al.*, Eur. Phys. J. A **7**, 421 (2000).
  - [20] A. Afanasev, I. Akushevich, and N. Merenkov, Phys. Rev. D **64**, 113009 (2001).
  - [21] J. Friedrich and Th. Walcher, Eur. Phys. J. A **17**, 607 (2003).
  - [22] B. Anderson *et al.*, Phys. Rev. C **75**, 034003 (2007) and references therein.
  - [23] S. Platchkov *et al.*, Nucl. Phys. **A510**, 740 (1990).
  - [24] R. Schiavilla and I. Sick, Phys. Rev. C **64**, 041002(R) (2001).
  - [25] D.I. Glazier *et al.*, Eur. Phys. J. A **24**, 101 (2005).